PHILOSOPHICAL TRANSACTIONS OF THE ROYAL SOCIETY A MATHEMATICAL, PHYSICAL & ENGINEERING SCIENCES

Size distributions of 3–10 nm atmospheric particles: implications for nucleation mechanisms

Peter H. McMurry, Keung Shan Woo, Rodney Weber, Da-Ren Chen and David Y. H. Pui

Phil. Trans. R. Soc. Lond. A 2000 **358**, 2625-2642
doi: 10.1098/rsta.2000.0673

10.1098/rsta.2000.0673

THE ROYAL SOCIETY

Size distributions of 3–10 nm atmospheric particles: implications for nucleation mechanisms

By Peter H. McMurry[1], Keung Shan Woo[1], Rodney Weber[2], Da-Ren Chen[1] and David Y. H. Pui[1]

[1]*125 Mechanical Engineering, University of Minnesota, 111 Church Street S.E., Minneapolis, MN 55455, USA*

[2]*School of Earth and Atmospheric Sciences, Georgia Institute of Technology, 221 Bobby Dodd Way, Atlanta, GA 30332, USA*

The formation of new atmospheric particles by gas-to-particle conversion leads to enhanced concentrations of nanoparticles. We have studied the formation and growth of new particles in urban Atlanta and in the remote atmosphere in locations ranging from the North Pole to Mauna Loa, Tasmania and the South Pole. Key to this work was our development of new measurement techniques for freshly formed nucleation mode particles between 3 and 10 nm. In this paper we show that measured aerosol size distributions in the 3–10 nm diameter range often increase with decreasing size down to our minimum detectable size of 3 nm, presumably because nucleation was occurring during the measurement. Furthermore, we show that the Atlanta nucleation mode size distributions are consistent with a collision-controlled nucleation process in which accommodation coefficients for all collisions between condensing molecules and molecular clusters and between molecular clusters are assumed to be equal to one, and in which evaporation from molecular clusters is neglected, as would be expected for a highly supersaturated vapour.

Keywords: atmospheric aerosol; ultrafine aerosol; homogeneous nucleation; sulphuric acid; nanoparticles; nucleation mode; gas-to-particle conversion

1. Introduction

The recent development of instrumentation for measuring particles as small as 3 nm (see, for example, Stolzenburg & McMurry 1991; Winklmayr *et al*. 1991; Saros *et al*. 1996; Reischl *et al*. 1997; Chen *et al*. 1998) has led to the discovery of a new mode of atmospheric particles in the nanometre size range (Covert *et al*. 1996*a*). We refer to these 3–10 nm particles as 'nucleation mode' aerosols, as they are almost certainly produced by recent nucleation from the gas phase. Other modes that have been previously documented include the nuclei or Aitken mode (typically *ca*. 20–50 nm mean size), the accumulation mode (between 0.1 and 1.0 μm) and the coarse particle mode (greater than 1 μm) (Whitby 1978). This paper briefly describes the instruments that we have developed and used to measure nucleation mode aerosols and discusses some results of those measurements in urban Atlanta and in the remote troposphere.

Nucleation mode aerosols have been observed in several characteristic situations in a wide variety of locations. The appearance of 3–10 nm particles sometimes follows

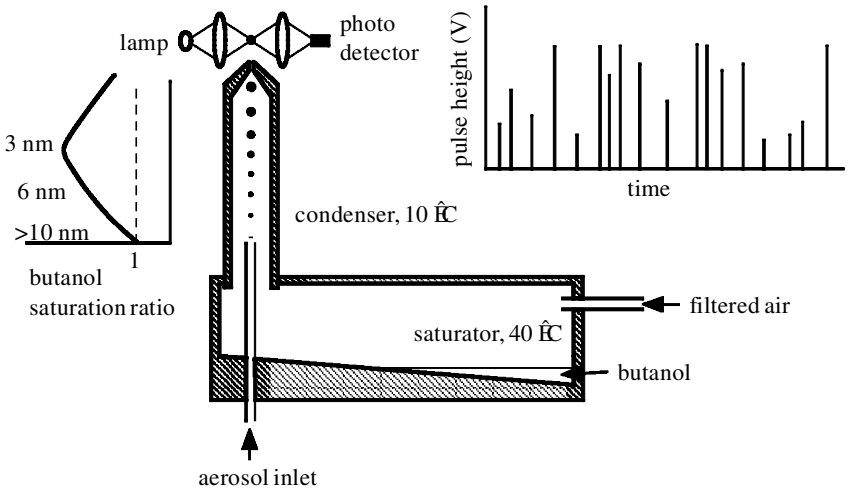

Figure 1. Schematic of the UCPC-PHA instrument. The alcohol saturation ratio required to initiate condensational growth increases sharply with decreasing size below 10 nm. Therefore, small particles must travel further into the condenser before they begin to grow, and they grow to a smaller ultimate size. The initial particle size is inferred from measurements of the final droplet size measured with the white light optical detector.

regular diurnal patterns, with peak particle production rates occurring near midday, when solar radiation is most intense (Bradbury & Meuron 1938; Went 1964; Hogan 1968; Koutsenogii & Jaenicke 1994). At other times, nucleation occurs in response to atmospheric perturbations, such as the removal of pre-existing aerosol by cloud processing (Hegg *et al*. 1990; Radke & Hobbs 1991; Perry & Hobbs 1994; Clarke *et al*. 1998) or the addition of gas phase reactants from a surface source. For example, measurements downwind of the coast at Mace Head, Ireland, have shown the rapid production of exceedingly high concentrations of very small particles during on-shore flow (McGovern *et al*. 1996; McGovern 1999). These events occur only in sunlight and during low tide. Nucleation was also detected in the remote marine atmosphere downwind of penguin colonies on Macquarie Island (Weber *et al*. 1998*a*). Weber and co-workers hypothesized that new particles were produced when ammonia, or perhaps some other gas emitted by these colonies, reacted with sulphuric acid that was present in the air flowing over the island to produce new particles. Nucleation has been observed on mountains (Shaw 1989; Marti 1990; Weber *et al*. 1995, 1997; Raes *et al*. 1997; Wiedensohler *et al*. 1997), in the boreal forests of Finland (Mäkelä *et al*. 1997; Kulmala *et al*. 1998) and in northern Finland (Pirjola *et al*. 1998) and in moderately polluted continental air in Germany (Birmili & Wiedensohler 1998). Measurements of aerosol composition suggest that the freshly nucleated particles in the Finnish boreal forest are enriched with dimethyl amine (Mäkelä *et al*. 1999). Evidence of nucleation in the marine boundary layer (MBL) has been reported (Covert *et al*. 1992; Hoppel *et al*. 1994; Clarke *et al*. 1998). Several groups (Covert *et al*. 1996*a*, *b*; Wiedensohler *et al*. 1996) have argued that nucleation mode particles detected in the MBL are probably produced aloft in free tropospheric cloud outflows and transported to the surface. Evidence suggests that nucleation in the upper tropical troposphere is a significant global source of atmospheric particles (Clarke 1993; Brock *et al*. 1995; Clarke *et al*. 1998).

While nucleation in a wide variety of circumstances is now well documented, we do not yet have validated models for predicting nucleation rates. Evidence suggests that sulphuric acid vapour may often participate in nucleation (Eisele & McMurry 1997; Clarke *et al*. 1998). Observed nucleation rates are occasionally consistent with predictions of the binary theory for sulphuric acid and water (Weber *et al*. 1999), but rates of particle formation are often orders of magnitude higher than can be explained by the binary theory. Furthermore, growth rates of freshly nucleated particles are typically two to ten times higher than can be explained by the condensation of sulphuric acid and its associated water and ammonia (Weber *et al*. 1996, 1997, 1998*a*, 1999).

The present paper reports on measurements of freshly nucleated 3–10 nm aerosol size distributions. We show that in systems where nucleation is occurring or has recently occurred, size distributions exhibit an increasing trend with decreasing particle size. Our measurements were made possible by our development of new instrumentation for measuring size distributions in the 3–10 nm diameter range. We also show that 3–10 nm size distributions measured in Atlanta are consistent with the theoretical predictions for collision-controlled nucleation.

2. Advances in instrumentation

The measurements described in this paper use two different instruments for measuring nucleation mode size distributions: the ultrafine condensation particle counter pulse height analysis method (UCPC-PHA) (Saros *et al*. 1996) and the nanometre scanning mobility sizer (nano-SMPS). The nano-SMPS uses the new nano-DMA (Chen *et al*. 1998) to classify particles according to electrical mobility. In this section we briefly summarize the relative strengths of these techniques.

The UCPC-PHA technique uses the instrument described by Stolzenburg & McMurry (1991), the prototype of the TSI 3025 UCPC. A schematic of this instrument is shown in figure 1. The sampled aerosol enters the condenser, where it is surrounded by an annular filtered sheath flow that has been saturated with butanol at 40 °C. Because the flow in the condenser is laminar, the particles remain on axis as they flow through it. The butanol rapidly diffuses into the aerosol, where it becomes supersaturated as a result of heat transfer from the 10 °C walls. Saturation ratios along the axis increase from the inlet value of 1.0 until, due to condensation on the cool walls, they decrease after reaching a peak value about two-thirds of the way through the condenser. The saturation ratio that is required to initiate condensational growth increases with decreasing size due to the effect of curvature on equilibrium vapour pressure (Thomson 1871). The highest saturation ratio that is achieved in the condenser is sufficient to initiate condensational growth on *ca.* 3 nm particles, but these particles have a relatively short time to grow. Growth of larger particles is activated at lower saturation ratios. The final droplet size at the exit from the condenser decreases with decreasing growth time. Therefore, very small particles grow to a smaller final droplet size and scatter less light than do larger particles. The PHA technique involves measuring the voltage pulses produced by individual droplets as they flow through the optical detector. The measured distribution of pulse heights can be inverted to obtain information about size distributions in the 3–10 nm diameter range (Weber *et al*. 1998*b*).

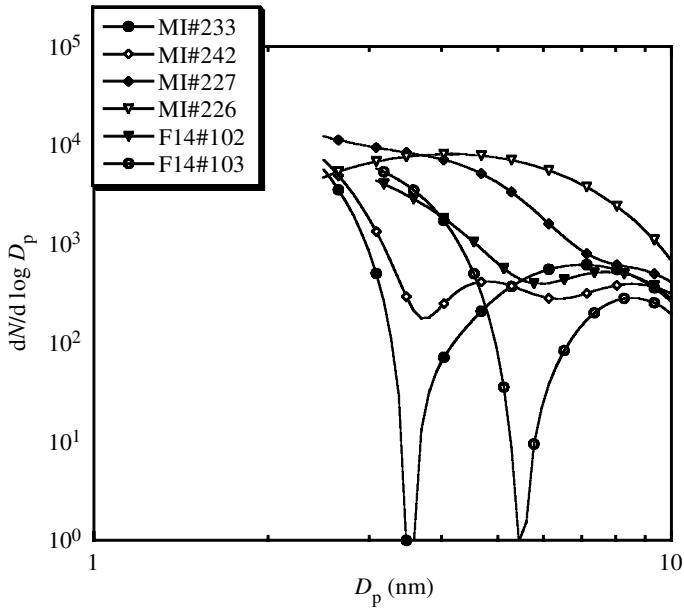

Figure 2. Examples of nucleation mode size distributions measured with the UCPC-PHA in the remote marine troposphere. The symbols on the curves are shown to identify the measurements, and do not correspond to 'size bins' for the PHA-UCPC.

The advantage of the UCPC-PHA technique is that all 3–10 nm particles in the sampled flow are detected. This enables fast measurements at very low concentrations. The lower limit on concentration is determined by counting statistical uncertainties. The aerosol flow rate is 0.5 $\mathrm{cm}^3\ \mathrm{s}^{-1}$. The number of nanoparticles counted, therefore, is

$$C_{3\text{–}10} = 0.5 N_{3\text{–}10} t, \tag{2.1}$$

where $N_{3\text{–}10}$ is the number concentration of 3–10 nm diameter particles and t is the counting time in seconds. The Poisson counting statistical uncertainty varies as the square root of the number of counts. If we assume that particle counts are equally distributed among 10 size (pulse height) bins, then the relative uncertainty in any one bin is, approximately,

$$\left(\frac{\Delta C}{C}\right)_{\text{PHA Bin}} \approx \left(\frac{20}{N_{3\text{–}10} t}\right)^{0.5}. \tag{2.2}$$

Assuming that an acceptable relative uncertainty for measurements is *ca.* 10%, it follows that

$$N_{3\text{–}10} t \geqslant 2000\ \mathrm{cm}^{-3}\ \mathrm{s}^{1}. \tag{2.3}$$

Therefore, a typical counting time of 20 s permits measurements of 3–10 nm size distributions when $N_{3\text{–}10}$ exceeds *ca.* 100 cm^{-3}. Coincidence errors occur when more than one particle is simultaneously present in the optical detector, and this happens when total concentrations of all particles exceed *ca.* 4000 cm^{-3}. It is necessary to dilute the aerosol prior to measurement when sampling aerosols with concentrations higher than this.

The nano-SMPS was designed for optimal measurements of electrical mobility distributions of particles in the 3–50 nm diameter range. This instrument system consists of a TSI 3080N nano-DMA with a TSI 3025 UCPC detector. For the measurements discussed in this paper, aerosols are exposed to a bipolar ion cloud, where they are brought to a known charge distribution (Wiedensohler 1988). At the exit from this bipolar charger, 1.27% of 3 nm particles and 5.03% of 10 nm diameter particles contain −1 elementary charges. The aerosol then is classified according to electrical mobility by the nano-DMA and counted with the UCPC, which samples at 0.5 $\mathrm{cm}^3\ \mathrm{s}^{-1}$ downstream of the nano-DMA. The relationship between the concentration detected by the UCPC and the size distribution for particles much smaller than the mean free path of air is (Knutson 1976)

$$N_{\mathrm{UCPC}} \approx 0.5 f_{\mathrm{aerosol}} \varphi \frac{\mathrm{d}N}{\mathrm{d}\ln D_{\mathrm{p}}} \approx 0.5 f_{\mathrm{aerosol}} \varphi \frac{N_{3\text{–}10}}{\ln(10/3)}, \tag{2.4}$$

where f_{aerosol} is the ratio of the aerosol to sheath air flow rates into and out of the nano-DMA, φ is the fraction of aerosol at a given size that carries an elementary charge, and $\mathrm{d}N/\mathrm{d}\ln D_{\mathrm{p}}$ is the value of the measured aerosol size distribution function. Using arguments similar to those discussed previously for the UCPC-PHA technique, we conclude that measurements providing 10% accuracy at a given nano-DMA classifying voltage will be obtained when

$$\begin{aligned} N_{3\text{–}10} t_{\text{nano-DMA voltage setting}} &\geqslant \frac{5000}{\varphi}\ \mathrm{cm}^{-3}\ \mathrm{s}, \\ &\sim 3.7 \times 10^5\ \mathrm{cm}^{-3}\ \mathrm{s} \quad \text{(for 3 nm particles)}, \\ &\sim 1.0 \times 10^5\ \mathrm{cm}^{-3}\ \mathrm{s} \quad \text{(for 10 nm particles)}. \end{aligned} \tag{2.5}$$

The total time required to measure the size distribution between 3 and 10 nm varies in proportion to the number of DMA classifying voltages employed. Thus, for a given counting time the UCPC-PHA can measure size distributions that are about a factor of 500–1000 times lower than can be measured with the nano-DMA. However, the time response of the nano-DMA could be improved by about a factor of five to ten by using a higher flow-rate detector, and an additional factor of ten by using a unipolar charger in place of the bipolar charger (Chen & Pui 1999).

The sizing resolution of the nano-DMA is superior to that of the UCPC-PHA. For example, laboratory calibrations with monodisperse calibration aerosols show that particles that vary by ±50% in diameter can produce the same pulse height with the UCPC-PHA. In contrast, particles that vary by about ±4% in diameter will exit the nano-DMA at a given classifying voltage under operating conditions used in our studies. Therefore, the nano-DMA is the instrument of choice if concentrations are sufficiently high to permit measurements in a reasonable period of time. Because the UCPC-PHA can rapidly measure size distributions at low concentrations, it has advantages for measurements in the clean troposphere.

3. Tropospheric measurements

We have used the PHA-UCPC to study nucleation in the remote marine and continental troposphere. The PHA-UCPC measurements were done as part of short-term (four to six weeks) intensive field programmes at locations including the Arctic Ocean

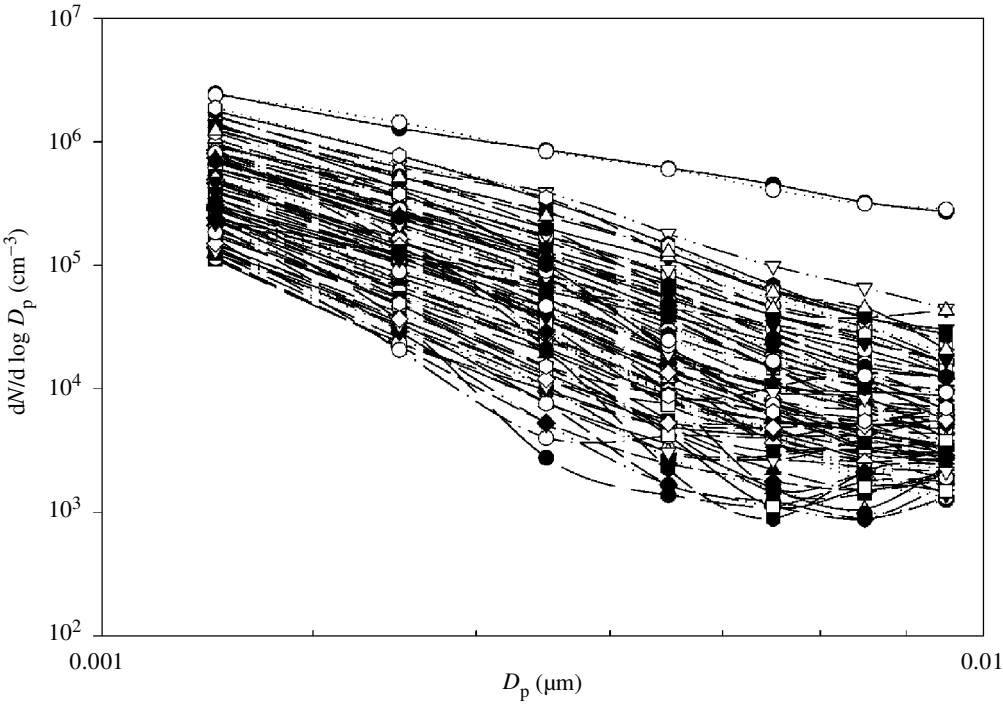

Figure 3. Nucleation mode size distributions measured with the nano-DMA in urban Atlanta, GA. These measurements represent all data during a one-year period where significant concentrations of 3–10 nm particles were present.

(Covert *et al*. 1996*a*), Mauna Loa, HI (Weber *et al*. 1995), the Rocky Mountains of Colorado (Weber *et al*. 1997), the South Pole and over the Southern Ocean during ACE-1 (Weber *et al*. 1998*a*, 1999). Examples of nucleation mode size distributions measured over the Southern Ocean are shown in figure 2. The data labelled 'MI' were measured downwind of Macquarie Island, the site of a large penguin colony. Distributions 233 and 242 were measured *ca*. 1 km downwind of the island, and distributions 227 and 226 were measured 21 and 32 km downwind respectively. We believe nucleation occurred during these measurements when marine air entrained emissions (possibly ammonia or amines) from the island. Distributions 102 and 103 were measured in the outflow regions of convective clouds.

Several interesting features can be observed in the size distribution functions shown in figure 2. Most significantly, observed distributions often increase with decreasing diameter at the bottom end of our measurement range, especially shortly after nucleation is first observed. For example, distributions 233 and 242, which were measured immediately downwind of Macquarie Island, show a pronounced increasing trend with decreasing size. We believe this is because nucleation was occurring during our measurements, and there was a continual flux of particles into the measured size range at these times. This rising trend often disappeared after nucleation had proceeded for some time (see, for example, distribution 226). The sharp minima in several of the distributions are also intriguing. Due to inherent limits in size resolution of the UCPC-PHA technique, we are not absolutely certain these minima are real. However, our analyses suggest that it should be possible to recover such minima

when inverting UCPC-PHA data (Weber *et al*. 1998*b*). Furthermore, it will be shown in the following section that theory shows such minima can occur during nucleation.

The nano-DMA was used to measure size distributions of 3–50 nm particles in Atlanta (Woo *et al*. 2000). In this study we also used a conventional SMPS for particles between 20 and 250 nm, and a PMS LASAIR optical particle counter for particles between 0.1 and 2 μm. These measurements are being carried out as part of the ARIES aerosol health-effects experiment. Measurements began in August 1998, and size distributions have been measured every 12 min all year round. During the first year of this study we measured 85 hourly-average size distributions that increased with decreasing size in the 3–10 nm diameter range. These size distributions are shown in figure 3.

The data in figure 3 exhibit several interesting features. Size distributions again increase with decreasing size down to our minimum detectable size, suggesting that nucleation was occurring. Also, while the magnitudes of the distributions vary by about a factor of 10 at any given size, the slopes are quite linear with a mean value of −3.5 and fall within the range,

$$-1.19 > \frac{\mathrm{d}}{\mathrm{d}\log D_\mathrm{p}} \log\left(\frac{\mathrm{d}N}{\mathrm{d}\log D_\mathrm{p}}\right) > -5.64. \tag{3.1}$$

The magnitudes of the nucleation mode distribution functions measured in Atlanta exceed those measured in the remote troposphere by typically one to two orders of magnitude. As with the distributions measured in the remote troposphere, minima are occasionally observed, although the minima for Atlanta tend to occur at somewhat larger sizes and are not as pronounced.

4. Discussion

In previous work we calculated numerically time-dependent size distributions of nucleation mode aerosols in systems where a condensable species (the 'monomer') is produced at a constant rate, R. The calculations take account of monomer production by gas phase chemical reactions, condensation of monomer on newly formed molecular clusters and on pre-existing aerosol, coagulation between molecular clusters, evaporation of monomer from molecular clusters, and coagulation between molecular clusters and pre-existing aerosol. Following the approach typically used with nucleation theory, we assumed that evaporation rates can be calculated using the capillarity approximation. We assumed that the size distribution of the pre-existing aerosol is not significantly altered by condensation during the nucleation event, and that the mass accommodation coefficient of monomer on pre-existing aerosol or molecular clusters equals one, which is justified by both theory and measurement (Clement *et al*. 1996; Jefferson *et al*. 1997). These analyses showed that the time-dependent nucleation mode size distributions depend on three dimensionless variables, E, A and L, defined as

$$E = N_\mathrm{s}\left(\frac{\beta_{11}}{R}\right)^{1/2}, \tag{4.1}$$

$$A = 4\left(\frac{\pi}{6}\right)^{1/3} \frac{v_1^{2/3}\sigma}{k_\mathrm{B}T}, \tag{4.2}$$

$$\sqrt{L} = \left(\frac{k_B T}{2\pi m_1}\right)^{1/2} \frac{I}{\sqrt{\beta_{11} R}}. \tag{4.3}$$

Variables are defined in the nomenclature. The parameters E and A determine the significance of monomer evaporation (Rao & McMurry 1989); calculated distribution functions are highly sensitive to these parameters. The surface tension parameter A depends only on temperature and properties of the condensing species. For systems in which the vapour is produced at a very high rate (i.e. R is large) or for which the monomer saturation vapour pressure is small (N_s is very small), E approaches zero and the monomer evaporation terms become negligible. We refer to this as the 'collision-controlled regime'. McMurry (1980) found that total number concentrations and size distributions of aerosols larger than 10 nm produced by the photo-oxidation of SO_2 in smog chambers at reaction rates exceeding *ca.* 10^6 molecules $cm^{-3}\ s^{-1}$ are in good agreement with predictions of the collision-controlled theory. L determines the significance of monomer condensation and the coagulation of freshly formed particles onto pre-existing aerosol (McMurry 1983). Note that $\sqrt{L}$ varies in proportion to the Fuchs integral, I, which equals the aerosol surface area for particles that are much smaller than the gas mean free path. For typical transition regime atmospheric aerosols, the Fuchs integral is a bit smaller than the surface area. Although atmospheric nucleation is undoubtedly heteromolecular, this theory treats the process as a quasi-single-component process, with the growth or evaporation of the molecular clusters rate limited by a single, low-vapour-pressure species.

Figure 4 shows calculated size distributions as a function of the heterogeneous loss parameter, L, for collision-controlled nucleation ($E = 0$). The results shown are dimensionless. The relationship between the dimensional and dimensionless size variables is

$$\left.\frac{dN}{d\log D_p}\right|_{\text{dimensional}} = \left(\frac{R}{\beta_{11}}\right)^{1/2} \left.\frac{d\tilde{N}}{d\log \tilde{D}_p}\right|_{\text{dimensionless}}, \tag{4.4}$$

$$D_p|_{\text{dimensional}} = v_1^{1/3} \tilde{D}_p|_{\text{dimensionless}}. \tag{4.5}$$

The analysis shows that size distributions rapidly achieve a steady state that depends on L, and it is these steady state results that are shown in figure 4. The vertical lines in figure 4 show the 3–10 nm window corresponding to the range of data shown in figures 2 and 3. These dimensional sizes were obtained from equation (4.5) assuming a monomer volume of $v_1 \cong 3 \times 10^{-22}\ cm^3$. This corresponds approximately to the molecular volume of sulphuric acid and its associated water at 50% relative humidity, and is slightly smaller than the volume of a molecule of $(NH_4)_2SO_4$. Because dimensionless size varies as $v_1^{1/3}$, it is not necessary to know v_1 precisely. Note that the slopes of the distribution functions become steeper as L increases. The calculated distribution functions have slopes of -2.38 for $L = 0.56$, and -6.56 for $L = 2.0$. These slopes are in the range of the values measured in Atlanta (figure 3).

Figure 5 shows calculated steady-state size distributions as a function of the evaporation parameter E for $L = 0.58$ and $A = 8$. This value of A is typical of values that would be expected for organics but is smaller than the characteristic value for sulphuric acid ($A \sim 16$). Calculations were done using $A = 8$ because the equations became exceedingly stiff and difficult to solve for larger values of A. The value $L = 0.58$ corresponds approximately to the lowest value that can occur. It is the value

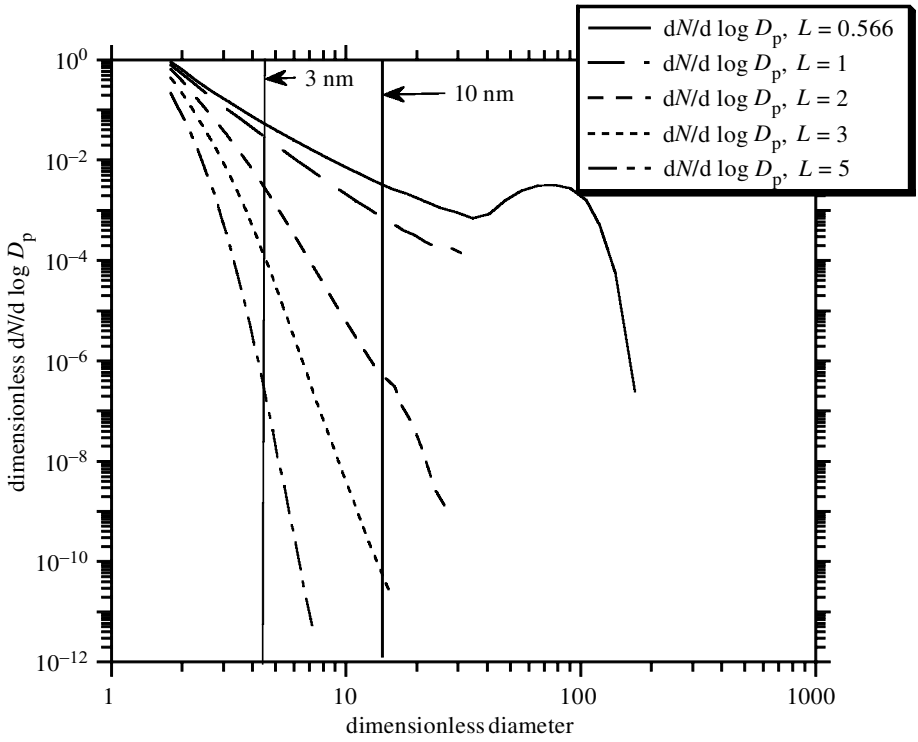

Figure 4. Calculated steady-state aerosol size distributions when condensable vapour is produced at a constant rate in a collision-controlled system. The parameter L increases with increasing aerosol surface area of particles larger than *ca.* 10 nm.

that is produced for a system initially free of particles, and reflects loss of monomer and clusters to particles larger than *ca.* 10 nm that were produced by nucleation. Note that size distributions are highly sensitive to E for $E > 0.02$. Also, for large values of E, minima are predicted for particles in the 3–10 nm diameter range. These trends would be even more pronounced for larger values of A. The size distributions for values of E up to 0.02 are qualitatively consistent with observed size distributions in Atlanta. The measured size distributions are quite different from size distributions calculated for larger values of E, however. The size distributions observed for larger values of E might be consistent with the PHA-UCPC measurements in the remote troposphere (figure 2).

If we assume that nucleation is collision-controlled, two approaches can be used to find the monomer production rate, R, for the Atlanta data (figure 3). The slope of the measured distribution function provides a value for the dimensionless scavenging rate parameter, L (see figure 4). R is then evaluated from equation (4.3), where the Fuchs integral, I, is calculated from measured size distributions. We refer to this value of R as R_L. Alternatively, the slope of the measured size distribution is used to find the value of the dimensionless size distribution at the minimum detectable size (see figure 4), and the value of R that scales the dimensionless to the dimensional size distribution is evaluated from equation (4.4). We refer to this value of R as R_{scale}. R_L and R_{scale} are compared in figure 6. As was shown in figure 3, most of the size distributions measured in Atlanta had linear slopes, but some did not. The open

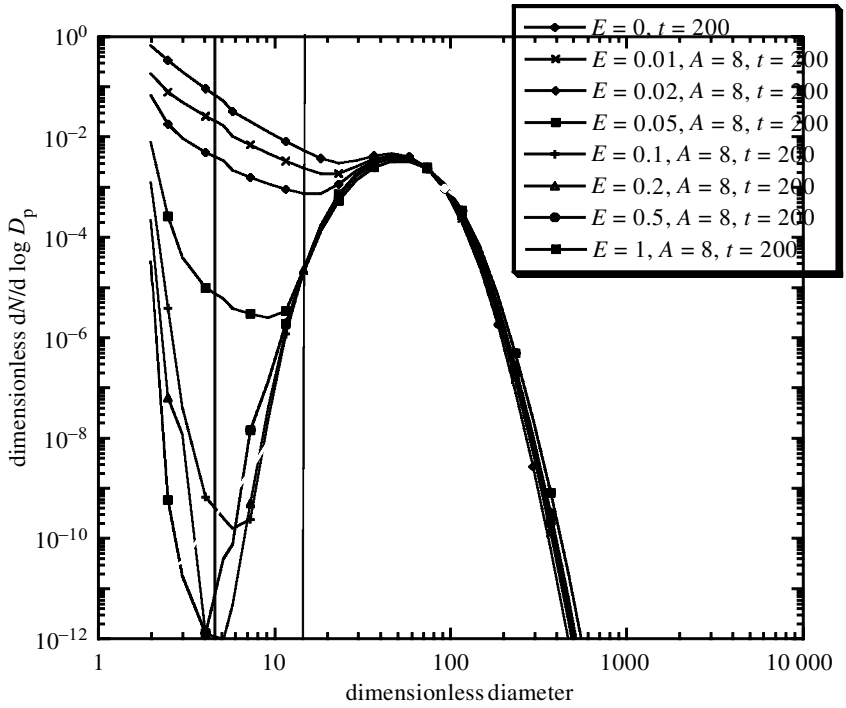

Figure 5. Calculated steady-state aerosol size distributions for several values of the evaporation parameter E. Calculations were done using $A = 8$ and $L = 0.58$.

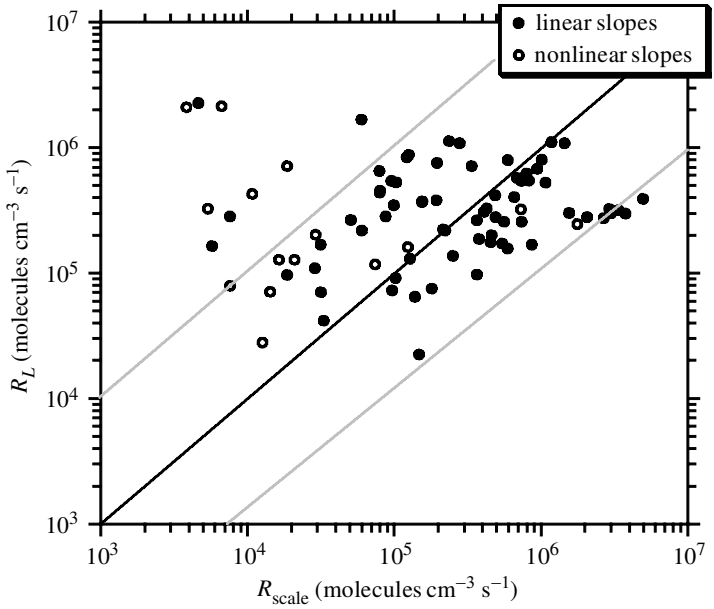

Figure 6. Comparison of monomer production rates for Atlanta calculated in two different ways. Calculations assume that nucleation is collision-controlled.

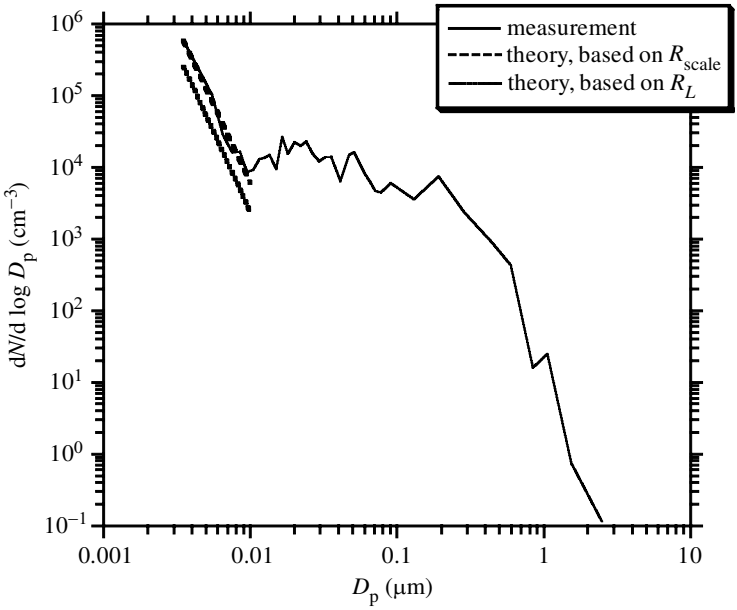

Figure 7. Comparison of measured and theoretical size distributions for 3–10 nm aerosols for one typical Atlanta measurement. The theory assumes collision-controlled nucleation ($E = 0$). Theoretical results are shown for the monomer production rate, R, calculated in two different ways.

circles in figure 6 apply to data with nonlinear slopes. Note that for *ca.* 90% of our measurements, the values of R calculated in these ways agreed to within a factor of 10. Several of the outliers apply to measurements with nonlinear slopes. Several of these measurements were made early in the morning or late in the evening, when the assumption that nucleation mode aerosol size distributions are at steady state would be invalid. The values of R determined by these two approaches are not systematically different, although there is significant scatter. Measured and theoretical collision-controlled (i.e. $E = 0$) size distributions are shown for one typical measurement in figure 7. Theoretical size distributions corresponding to the values of R_L and R_{scale} obtained for this measurement (2.5×10^5 molecules cm^{-3} s^{-1} and 5.7×10^5 molecules cm^{-3} s^{-1}, respectively) are shown.

The results shown in figures 6 and 7 are based on the assumption that nucleation in Atlanta was collision-controlled. A more rigorous testing of this hypothesis would require solutions of the cluster balance equations for $E > 0$ over a wider range of L and for values of A applicable to the nucleating aerosols; the results shown in figure 5 were done for L=0.58, and we have not carried out calculations for other values of L. However, if the results in figure 5 are characteristic of those for other values of L, it would appear unlikely R_L and R_{scale} would have been comparable in magnitude (figure 6) if evaporation from clusters had played a significant role. The results of figure 5 show that slopes of the distribution are comparable for $E = 0$, $E = 0.01$ and $E = 0.02$, but the 3.5 nm intercepts vary by more than a factor of ten. If the true value of E had been 0.02 (rather than 0 as was assumed above), then R_{scale} would have been more than a factor of 100 higher than was found for collision-controlled nucleation ($E = 0$). It is likely that this discrepancy would be even larger

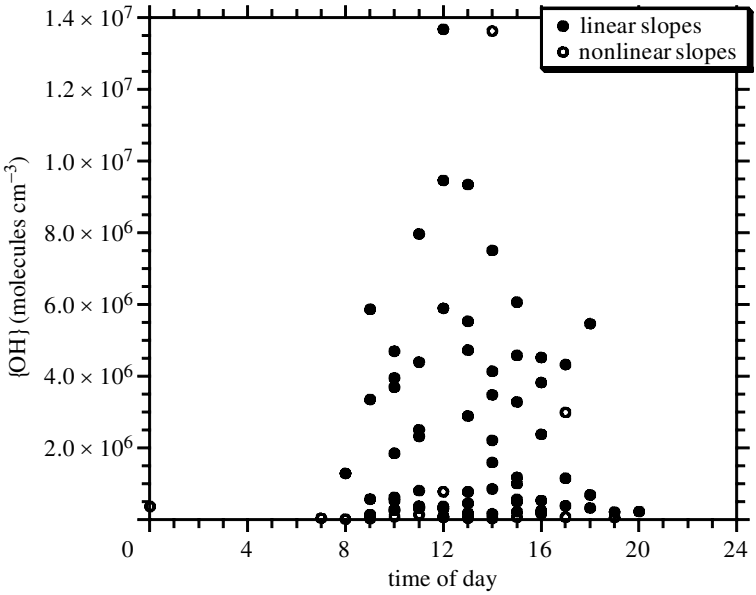

Figure 8. Hydroxyl radical concentrations required to produce calculated monomer production rates for measured concentrations of sulphur dioxide.

if calculations had been done for larger values of A and L, as might be appropriate for these atmospheric aerosols. Because the slopes of these curves are similar, however, R_L would be changed by only a small amount. Therefore, values of E as small as 0.01 or 0.02 would have led to $R_{\text{scale}} \gg R_L$. The results shown in figure 6 show that this is not the case. Furthermore, for values of $E > 0.02$, theory shows that the slope of the distribution function would not have been linear as was experimentally observed in Atlanta, further supporting our argument that nucleation was collision-controlled. The remote tropospheric distribution functions (figure 3), however, do not have linear slopes. This could reflect the importance of cluster evaporation during these measurements. In order to explain such size distributions with theory, it will be necessary to fit the measured distribution function to a theoretical function that is similar in shape. We have not yet attempted to do this.

It is instructive to speculate on species that might be responsible for the observed nucleation. For collision-controlled nucleation, the dimensionless monomer concentration is insensitive to L, ranging from 0.58 for $L = 0.6$ to 0.49 for $L = 2$ (McMurry 1983). As an approximation we assume a typical value of 0.5. The monomer concentration is therefore (McMurry 1983)

$$N_1 = 0.5\left(\frac{R}{\beta_{11}}\right)^{0.5} \approx 2.24 \times 10^4 \sqrt{R} \text{ molecules cm}^{-3}. \tag{4.6}$$

Based on the values of R shown in figure 6 (similar results are obtained with either R_L or R_{scale}), we find that N_1 falls below 1.2×10^7 molecules cm^{-3} for 50% of our measurements and below 2.2×10^7 molecules cm^{-3} for 90% of our measurements. Based on our previous studies (see, for example, Eisele & McMurry 1997), we believe that sulphuric acid may participate in nucleation. Sulphuric acid vapour was not measured during the Atlanta study. In our previous studies in the remote

troposphere, however, sulphuric acid vapour concentrations measured during nucleation events occasionally reached levels as high as 2×10^7 molecules cm^{-3} (Weber *et al.* 1996), but covered the range $1 \times 10^4 < [H_2SO_4] < 2 \times 10^7$ molecules cm^{-3} with an average value of *ca.* 1×10^6 molecules cm^{-3}. Thus, the calculated monomer concentrations for collision-controlled nucleation in Atlanta are somewhat higher (up to a factor of 10) than the sulphuric acid concentrations that have been measured in the remote troposphere when nucleation is occurring. If similar species were involved with nucleation in both locations, then the evaporation terms in the cluster balance equations would certainly be less significant in Atlanta since the supersaturation of the nucleating species was approximately a factor of ten higher. It is likely that other species that participate in nucleation (ammonia, amines, etc.) are more abundant in Atlanta than in the urban troposphere. This could also lead to reduced sulphuric acid vapour pressures and lead to nucleation that is more nearly collision-controlled.

An upper limit for the saturation vapour concentration of the condensing species, N_s, can be estimated from equation (4.1). Based on the above arguments, we assume that during nucleation in Atlanta, the E was less than 0.01. Because 90% of the calculated monomer production rates, R_{scale}, were below 1.3×10^6 molecules cm^{-3} s^{-1}, we conservatively conclude that the saturation vapour concentration was below 5×10^5 molecules cm^{-3}. It would be equally justifiable to use a low value of R_{scale} to estimate the upper limit for N_s, since measured distribution functions were also found to be linear for small values of R_{scale}. We found that R_{scale} was below *ca.* 1.4×10^4 molecules cm^{-3} s^{-1} for *ca.* 10% of our observations. The corresponding upper limit for N_s is 5×10^4 molecules cm^{-3}. Saturation vapour concentrations of sulphuric acid vapour above solid ammonium sulphate aerosol particles of *ca.* 2.5×10^4 molecules cm^{-3} were reported by Marti *et al.* (1997). It follows that our calculated N_s values are in a reasonable range.

Another argument in support of the hypothesis that sulphuric acid participated in nucleation in Atlanta is our observation that sulphur dioxide concentrations were typically elevated during the nucleation events (Woo *et al.* 2000). To test the plausibility of the monomer production rates shown in figure 6, we have calculated the hydroxyl radical concentrations that would have been required to produce the calculated monomer production rates. The calculated hydroxyl radical concentrations were obtained from the following equation:

$$[OH] = \frac{R_{scale}}{8.5 \times 10^{-13}[SO_2]} \text{ molecules cm}^{-3}, \tag{4.7}$$

where $[SO_2]$ is the measured concentration of sulphur dioxide in molecules per cm^3 and the second-order rate constant for the SO_2–OH reaction is 8.5×10^{-13} cm^3 molecule^{-1} s^{-1} (DeMore *et al.* 1992). Values of [OH] calculated in this way are plotted versus time of day in figure 8. The calculated hydroxyl radical concentration follows a reasonable diurnal variation, with peak values occurring near noon. Half of the calculated hydroxyl concentrations are below *ca.* 8×10^5 molecules cm^{-3} and 90% are below *ca.* 8×10^6 molecules cm^{-3}. These values are in a reasonable range for an urban area (W. Chamiedes, personal communication), but hydroxyl radical concentrations have not been measured in the Atlanta atmosphere, and we have not attempted to compare our results with models applicable to our measurement periods.

5. Conclusions

Two instruments were used to measure size distributions of 3–10 nm diameter aerosols when nucleation was occurring. One of these systems (the UCPC-PHA), which measures the amount of light scattered by individual particles downstream of the condenser of an ultrafine condensation particle counter, is best suited for measurements where concentrations are low and measurements must be made quickly. For example, this instrument is well suited for aircraft measurements in the remote troposphere. The other system (the nano-SMPS) determines size with a new electrostatic classifier that was specially designed for particles as small as 3 nm and concentration with an ultrafine condensation particle counter. The nano-SMPS provides better sizing resolution than the UCPC-PHA but requires more time to complete a measurement. We used the nano-SMPS for measurements in Atlanta where concentrations were high and accurate measurements could be carried out in a few minutes.

Both instrument systems showed that aerosol size distribution functions increase with decreasing size at the minimum detectable particle size particle size (*ca.* 3 nm) when nucleation was occurring. We are not aware that this trend has been observed previously. Theory predicts that this should occur.

About 70 of the 85 observed hourly-averaged 3–10 nm diameter size distributions measured during nucleation in Atlanta over a period of one year can be expressed as

$$\frac{\mathrm{d}N}{\mathrm{d}\log D_\mathrm{p}} = A(D_\mathrm{p})^B; \qquad -5.64 < B < -1.19; \qquad B_\mathrm{average} = -3.5. \tag{5.1}$$

The magnitude of the distribution function at $D_p = 3.5$ nm (the midpoint of the smallest size range) ranged from *ca.* 10^5 to 2×10^6 cm^{-3}, which was one to two orders of magnitude higher than distribution functions measured in the remote troposphere. Also, the remote tropospheric distribution functions did not obey this simple functional relationship.

The Atlanta data are consistent with theoretical predictions for collision-controlled nucleation. The key assumptions of collision-controlled nucleation theory are that all condensing molecules stick together when they collide, and that evaporation from molecular clusters does not occur. We find that the monomer (i.e. condensing molecule) production rates that are required to produce the observed size distributions are in reasonable expectations with values that would be expected for the gas phase oxidation of sulphur dioxide by the hydroxyl radical. The collision-controlled analysis suggests that the vapour pressure of the condensing species is less than 50 000 molecules cm^{-3}.

Clearly, more work is required to verify the above hypotheses. It will be necessary to definitively identify the condensing species and to show experimentally that its concentration is equal to the value predicted theoretically. Furthermore, because the calculated monomer concentrations and equilibrium vapour concentrations are far below values that would be expected for sulphuric acid according to the classical binary theory, the process must involve species in addition to sulphuric acid and water. It is important that these species be identified.

Nomenclature

A surface tension parameter (see equation (4.2))

D_p particle diameter

E evaporation rate parameter (see equation (4.1))

I $$\frac{4\pi}{3}\int_{\substack{\text{pre-existing}\\ \text{aerosol}}} D_p^2\left(\frac{Kn+Kn^2}{1+1.71Kn+1.33Kn^2}\right)\frac{\mathrm{d}N}{\mathrm{d}\log D_p}\,\mathrm{d}\log D_p$$

k_B Boltzmann's constant

L dimensionless scavenging rate parameter (see equation (4.3))

m_1 monomer mass

N aerosol number concentration

N_s saturation concentration of nucleating vapour

R monomer production rate (molecules volume^{-1} time^{-1})

T temperature

v_1 monomer volume

Kn $2\lambda/D_p$

λ mean free path

β_{11} monomer collision frequency function

$$= 4\sqrt{2}\left(\frac{3}{4\pi}\right)^{1/6}\left(\frac{6k_BT}{\rho_p}\right)^{1/2} v_1^{1/6}$$

σ surface tension

This research was supported by EPRI Agreement WO9181-01 'Fine and Ultrafine Aerosol Size Distributions in Atlanta' and by DOE grant no. DE-FG02-98ER62556, 'Composition of Freshly Nucleated Aerosols'. We gratefully acknowledge this support.

References

Birmili, W. & Wiedensohler, A. 1998 The influence of meteorological parameters on ultrafine particle production at a continental site. *J. Aerosol Sci.* **29**, S1015–S1016.

Bradbury, N. E. & Meuron, H. J. 1938 The diurnal variation of atmospheric condensation nuclei. *Terr. Magn.* **43**, 231–240.

Brock, C. A., Hamill, P., Wilson, J. C., Honsson, H. H. & Chan, K. R. 1995 Particle formation in the upper tropical troposphere: a source of nuclei for the stratospheric aerosol. *Sci.* **270**, 1650–1653.

Chen, D.-R. & Pui, D. Y. H. 1999 A high efficiency, high throughput unipolar aerosol charger for nanoparticles. *J. Nanoparticle Res.* **1**, 115–126.

Chen, D. R., Pui, D. Y. H., Hummes, D., Fissan, H., Quant, F. R. & Sem, G. J. 1998 Design and evaluation of a nanometer aerosol differential mobility analyzer (nano-DMA). *J. Aerosol Sci.* **29**, 497–509.

Clarke, A. D. 1993 Atmospheric nuclei in the Pacific midtroposphere—their nature, concentration, and evolution. *J. Geophys. Res. Atmos.* **98**, 20 633–20 647.

Clarke, A. D. (and 14 others) 1998 Particle nucleation in the tropical boundary layer and its coupling to marine sulfur sources. *Science* **282**, 89–92.

Clarke, A. D., Varner, J. L., Eisele, F., Mauldin, R. L., Tanner, D. & Litchy, M. 1998 Particle production in the remote marine atmosphere: cloud outflow and subsidence during ACE 1. *J. Geophys. Res. Atmos.* **103**, 16 397–16 409.

Clement, C. F., Kulmala, M. & Vesala, T. 1996 Theoretical consideration on sticking probabilities. *J. Aerosol Sci.* **27**, 869–882.

Covert, A. D., Kapustin, V. N., Quinn, P. K. & Bates, T. S. 1992 New particle formation in the marine boundary layer. *J. Geophys. Res.* **97**, 20 581–20 589.

Covert, D. S., Wiedensohler, A., Aalto, P., Heintzenberg, J., McMurry, P. H. & Leck, C. 1996*a* Aerosol number size distributions from 3 to 500 nm diameter in the Arctic marine boundary layer during summer and autumn. *Tellus* B **48**, 197–212.

Covert, D. S., Kapustin, V. N., Bates, T. S. & Quinn, P. K. 1996*b* Physical properties of marine boundary layer aerosol particles of the mid-Pacific in relation to sources and meteorological transport. *J. Geophys. Res. Atmos.* **101**, 6919–6930.

DeMore, W. B., Sander, S. P., Golden, D. M., Hampson, R. F., Kurylo, M. J., Howard, C. J., Ravishankara, A. R., Kolb, C. E. & Molina, M. J. 1992 Chemical kinetics and photochemical data for use in stratospheric modeling, evaluation no. 10. *Jet Propulsion Laboratory* **92–20**.

Eisele, F. L. & McMurry, P. H. 1997 Recent progress in understanding particle nucleation and growth. *Phil. Trans. R. Soc. Lond.* B **352**, 191–201.

Hegg, D. A., Radke, L. F. & Hobbs, P. V. 1990 Particle production associated with marine clouds. *J. Geophys. Res.* **95**, 13 917–13 926.

Hogan, A. W. 1968 An experiment illustrating that gas conversion by solar radiation is a major influence in the diurnal variation of aitken nucleus concentrations. *Atmos. Environ.* **2**, 599–601.

Hoppel, W. A., Frick, G. M., Fitzgerald, J. & Larson, R. E. 1994 Marine boundary layer measurements of new particle formation and the effects nonprecipitating clouds have on aerosol size distribution. *J. Geophys. Res. Atmos.* **99**, 14 443–14 459.

Jefferson, A., Eisele, F. L., Ziemann, P. J., Weber, R. J., Marti, J. J. & McMurry, P. H. 1997 Measurements of the H_2SO_4 mass accommodation coefficient onto polydisperse aerosol. *J. Geophys. Res. Atmos.* **102**, 19 021–19 028.

Knutson, E. O. 1976 Extended electric mobility method for measuring aerosol particle size and concentration. In *Fine particles: aerosol generation, measurement, sampling, and analysis* (ed. B. Y. H. Liu), pp. 739–762. Academic Press.

Koutsenogii, P. K. & Jaenicke, R. 1994 Number concentration and size distribution of atmospheric aerosol in Siberia. *J. Aerosol Sci.* **25**, 377–383.

Kulmala, M., Toivonen, A., Makela, J. M. & Laaksonen, A. 1998 Analysis of the growth of nucleation mode particles observed in Boreal forest. *Tellus* B **50**, 449–462.

McGovern, F. M. 1999 An analysis of condensation nuclei levels at Mace Head, Ireland. *Atmos. Environ.* **33**, 1711–1723.

McGovern, F. M., Jennings, S. G. & Oconnor, T. C. 1996 Aerosol and trace gas measurements during the Mace Head experiment. *Atmos. Environ.* **30**, 3891–3902.

McMurry, P. H. 1980 Photochemical aerosol formation from SO_2: a theoretical analysis of smog chamber data. *J. Colloid Interface Sci.* **78**, 513–527.

McMurry, P. H. 1983 New particle formation in the presence of an aerosol: rates, time scales and sub-0.01 μm size distributions. *J. Colloid Interface Sci.* **95**, 72–80.

Mäkelä, J. M., *et al.* 1997 Observations of ultrafine aerosol particle formation and growth in boreal forest. *Geophys. Res. Lett.* **24**, 1219–1222.

Mäkelä, J., Mattila, T. & Hiltunen, V. 1999 *Measurement of the fine and ultrafine particle composition during the particle formation events observed at a boreal forest site.* Tacoma, WA: American Association for Aerosol Research.

Marti, J. 1990 Diurnal variation in the undisturbed continental aerosol: results from a measurement program in Arizona. *Atmos. Res.* **25**, 351–362.

Marti, J. J., Jefferson, A., Cai, X. P., Richert, C., McMurry, P. H. & Eisele, F. 1997 H_2SO_4 vapor pressure of sulfuric acid and ammonium sulfate solutions. *J. Geophys. Res. Atmos.* **102**, 3725–3735.

Perry, K. D. & Hobbs, P. V. 1994 Further evidence for particle nucleation in clear air adjacent to marine cumulus clouds. *J. Geophys. Res. Atmos.* **99**, 22 803–22 818.

Pirjola, L., Laaksonen, A., Aalto, P. & Kulmala, M. 1998 Sulfate aerosol formation in the Arctic boundary layer. *J. Geophys. Res. Atmos.* **103**, 8309–8321.

Radke, L. F. & Hobbs, P. V. 1991 Humidity and particle fields around some small cumulus clouds. *J. Atmos Sci.* **48**, 1190–1193.

Raes, F., Vandingenen, R., Cuevas, E., Vanvelthoven, P. F. J. & Prospero, J. M. 1997 Observations of aerosols in the free troposphere and marine boundary layer of the subtropical Northeast Atlantic: discussion of processes determining their size distribution. *J. Geophys. Res. Atmos.* **102**, 21 315–21 328.

Rao, N. P. & McMurry, P. H. 1989 Nucleation and growth of aerosol in chemically reacting systems: a theoretical study of the near-collision-controlled regime. *Aerosol Sci. Technol.* **11**, 120–132.

Reischl, G. P., Makela, J. M. & Necid, J. 1997 Performance of Vienna type differential mobility analyzer at 1.2–20 nanometer. *Aerosol Sci. Technol.* **27**, 651–672.

Saros, M. T., Weber, R. J., Marti, J. J. & McMurry, P. H. 1996 Ultrafine aerosol measurement using a condensation nucleus counter with pulse height analysis. *Aerosol Sci. Technol.* **25**, 200–213.

Shaw, G. E. 1989 Production of condensation nuclei in clean air by nucleation of H_2SO_4. *Atmos. Environ.* **22**, 2841–2846.

Stolzenburg, M. R. & McMurry, P. H. 1991 An ultrafine aerosol condensation nucleus counter. *Aerosol Sci. Technol.* **14**, 48–65.

Thomson, W. 1871 On the equilibrium of vapour at a curved surface of liquid. *Phil. Mag.* **42**, 448–453.

Weber, R. J., McMurry, P. H., Eisele, F. L. & Tanner, D. J. 1995 Measurement of expected nucleation precursor species and 3–500 nm diameter particles at Mauna Loa Observatory, Hawaii. *J. Atmos. Sci.* **52**, 2242–2257.

Weber, R. J., Marti, J., McMurry, P. H., Eisele, F. L., Tanner, D. J. & Jefferson, A. 1996 Measured atmospheric new particle formation rates: implications for nucleation mechanisms. *Chem. Engng Commun.* **151**, 53–64.

Weber, R. J., Marti, J. J., McMurry, P. H., Eisele, F. L., Tanner, D. J. & Jefferson, A. 1997 Measurements of new particle formation and ultrafine particle growth rates at a clean continental site. *J. Geophys. Res. Atmos.* **102**, 4375–4385.

Weber, R. J., *et al*. 1998*a* A study of new particle formation and growth involving biogenic trace gas species measured during ACE-1. *J. Geophys. Res.* **103**, 16 385–16 396.

Weber, R. J., Stolzenburg, M. R., Pandis, S. N. & McMurry, P. H. 1998*b* Inversion of ultrafine condensation nucleus counter pulse height distributions to obtain nanoparticle (similar to 3–10 nm) size distributions. *J. Aerosol Sci.* **29**, 601–615.

Weber, R. J., McMurry, P. H., Mauldin, L., Tanner, D., Eisele, F., Clarke, A. D. & Kapustin, V. N. 1999 New particle formation in the remote troposphere: a comparison of observations at various sites. *Geophys. Res. Lett. Atmos. Sci.* **26**, 307–310.

Went, F. W. 1964 The nature of Aitken condensation nuclei in the atmosphere. *Proc. Natn. Acad. Sci.* **51**, 1259–1266.

Whitby, K. T. 1978 The physical characteristics of sulfur aerosols. *Atmos. Environ.* **12**, 135–159.

Wiedensohler, A. 1988 An approximation of the bipolar charge distribution for particles in the submicron size range. *J. Aerosol Sci.* **19**, 387–389.

Wiedensohler, A., Covert, D. S., Swietlicki, E., Aalto, P., Heinzenberg., J. & Leck, C. 1996 Occurrence of an ultrafine particle mode less than 20 nm in diameter in the marine boundary layer during Arctic summer and autumn. *Tellus* B **48**, 289–296.

Wiedensohler, A. (and 15 others) 1997 Night-time formation and occurrence of new particles associated with orographic clouds. *Atmos. Environ.* **31**, 2545–2559.

Winklmayr, W., Reischl, G. P., Linder, A. O. & Berner, A. 1991 A new electromobility spectrometer for the measurement of aerosol size distribution in the size range from 1 to 1000 nm. *J. Aerosol Sci.* **22**, 289.

Woo, K. S., Chen, D.-R., Pui, D. Y. H. & McMurry, P. H. 2000 Measurements of Atlanta aerosol size distributrions: observations of ultrafine particle events. *Aerosol Sci. Technol.* (In the press.)

Discussion

R. M. Harrison (*Division of Environmental Health and Risk Management, University of Birmingham, UK*). As some of the molecules forming sulphuric acid clusters in the atmosphere could be small ions, what will be the effect of charge on cluster stability?

P. H. McMurry. Charged clusters are more stable than neutral ones. Therefore, ion-induced nucleation occurs at a higher rate than homogeneous nucleation of neutral species. However, I do not believe the concentration of ions would be high enough to explain the high rates of particle production we observed in the urban Atlanta atmosphere.

C. F. Clement (*Oxon, UK*). What has been used for the evaporation rate in the model described? Particularly with the smaller clusters, it is not obvious that only one molecule could be evaporated.

P. H. McMurry. As you point out, a primary difficulty in nucleation theory is calculating rates at which evaporation occurs from molecular clusters. If nucleation is collision controlled ($E = 0$), then evaporation is negligible relative to condensation and can be neglected. The data for the Atlanta atmosphere appear to be consistent with this hypothesis (i.e. that nucleation is collision controlled). For the theoretical results where evaporation was included ($E > 0$), evaporation rates were calculated by invoking the usual assumptions of classical nucleation theory: molecular clusters are assumed to have the same properties as the bulk liquid, the effect of curvature on vapour pressure is described by the Kelvin equation, and only individual molecules evaporate from clusters. I agree that this is a major area of uncertainty.

PHILOSOPHICAL TRANSACTIONS OF THE ROYAL SOCIETY A MATHEMATICAL, PHYSICAL & ENGINEERING SCIENCES